



NONLINEAR CONTROL OF MPPT AND GRID CONNECTED FOR VARIABLE SPEED WIND ENERGY CONVERSION SYSTEM BASED ON THE PMSG

¹Y.ERRAMI, ²M.HILAL, ³M.BENCHAGRA, ⁴M.OUASSAID, ⁵M.MAAROUFI

^{1,2,3,5}Department of Electrical Engineering, Mohammadia School of Engineering- Mohammed V-Agdal University, Rabat, Morocco

⁴Department of Industrial Engineering, Ecole Nationale des Sciences Appliquées-Safi, Cadi Ayyad University, Safi, Morocco

E-mail: ¹errami.emi@gmail.com, ²hilalisme@gmail.com, ³m.benchagra@gmail.com,
⁴ouassaid@emi.ac.ma, ⁵maaroufi@emi.ac.ma

ABSTRACT

The efficiency of the variable speed wind energy conversion systems (WECS) can be greatly improved using an appropriate control strategy. In this paper, nonlinear control for wind energy conversion system (WECS) based on the permanent magnet synchronous generator (PMSG) is investigated in order to maximize the generated power from wind turbine. The control strategy combines the technique of maximum power point tracking (MPPT) method and sliding mode (SM) nonlinear control theory, that as it is well known, presents a good performance under system uncertainties. The block diagram of the WECS with a back-to-back PWM converter structure and PMSG is established with the dq frame of axes. Considering the variation of wind speed, both converters used the sliding mode control scheme. The objectives of grid-side converter are to deliver the energy from the PMSG side to the utility grid, to regulate the DC-link voltage and to achieve unity power factor and low distortion currents, while a speed controller is designed to maximize the extracted energy from the wind, below the rated power area. Simulation results show the feasibility and robustness of the proposed control schemes for PMSG based variable speed wind energy conversion systems.

Keywords: *Lyapunov Theory, Sliding Mode Control, WECS, PMSG, MPPT, Unity Power Factor.*

1. INTRODUCTION

In recent years, the worldwide concern about the possible energy shortage and the environmental pollution has led to increasing interest in generation of renewable energy as it is a potential source for electricity generation with minimal environmental impact [1-2]. In addition, more and more importance is being attached to wind energy conversion system (WECS) that is growing at a faster rate than any other source energy. For economical and cleaner energy characteristics, the WECS are getting a lot of attention and they have been increasing rapidly [3-7]. In the WECS, wind turbine can operate with either variable speed or fixed speed. For fixed speed wind generation system, because of the generator is directly connected to the grid, the turbulence of the wind will result in power variations, and so affect the power quality in the grid, whereas for variable speed generation system, the generator is controlled

by power electronic converter[8-10]. So, variable speed wind energy conversion systems have many advantages over fixed speed generation, such as maximum power point tracking control method, increased power capture, power quality, improved efficiency and they can be controlled in order to reduce aerodynamic noise and mechanical stress [11-12]. In addition, with the development of power electronics technology, it's possible to control the rotor speed, to increase wind energy production and to reduce drive train loads. Thus the variable speed wind turbine generator system is becoming the most important and fastest growing application of wind generation system [12-18].

In terms of the generators for WECS, several types of electric generators are used such as Squirrel-Cage Induction Generator (SCIG), Synchronous Generator with external field excitation, Doubly Fed Induction Generator (DFIG) and Permanent Magnet Synchronous Generator (PMSG) with power electronic converter system [6-12]. Recently,

the use of the PMSG is becoming more and more common for several reasons such as: very high torque can be achieved at low speeds because PMSG is connected directly to the turbine without gearbox; lower operational noise is achieved; no significant losses are generated in the rotor and external excitation current is not needed. So, the efficiency of a PMSG based WECS has been assessed higher than other generators and PMSG is an attractive choice for variable-speed generation system [10-11], [15]. In the case of PMSG based WECS, because of the advance of power electronic technology, decreasing equipment costs, the integration of WECS and the large scale exploration, the PMSG interfaced to the grid with a full scale power converter is being increasingly adapted due to full controllability of the system and its higher power density. Moreover, in order to adjust the rotational speed to maximize the wind turbine PMSG output power from the fluctuating wind, variable speed operation of the system is necessary and, for various wind speeds, the wind turbine can be operate as close as possible to its optimal speed to realize maximum power point tracking (MPPT) [18-22]. Thus, control strategy for the WECS is used. In order to control the WECS, several control schemes have been proposed. Two controllers are used, one is the pitch controller for the pitch angle and the other one is the power controller regulating the output power. Therefore, there exists a variety of control schemes such as PI control [20-23]. They consist of two back-to-back PWM converters with a common dc-link. Control algorithm based on the vector control strategy has been investigated for both converters with PI control. Thus, decoupling control of active current and reactive current is necessary and active and active powers are controlled respectively by the inverter in grid-side [5-13]. Because of the PI control shows a limited performance, especially against uncertainties and can't follows the changes in system parameters, nonlinear control can be used in order to accommodate the effects of uncertainties and to provide better robustness. So, for power controller, [24-25] propose the nonlinear sliding mode control scheme below the rated wind speed in order to maximize the generated power and, [26-27] introduce high order sliding mode controllers in order to reduce the chattering effect. Recently, a sliding mode pitch control scheme is presented in [28].

In this paper, nonlinear control of MPPT and grid connected for variable speed WECS based on the PMSG is investigated in order to maximize the generated power with unity power factor. So, the

system under consideration includes a wind turbine generator, a PMSG, PWM rectifier in generator-side, intermediate DC link capacitor and PWM inverter in grid-side. The block diagram of proposed WECS is shown in Fig.1. In addition, WECS has strong nonlinear multivariable with many uncertain factors and disturbances. So the control strategy combines the technique of maximum power point tracking (MPPT) method and sliding mode (SM) nonlinear control, that, as it is well known, presents a good performance under system uncertainties [29-30]. A speed and pitch control scheme for WECS are proposed. Considering the variation of wind speed, both converters used the sliding mode control scheme. A speed controller is used in order to maximize the extracted energy from the wind, below the rated power area [16-20], while the objectives of grid-side converter are to deliver the energy from the PMSG side to the utility grid, to regulate the DC-link voltage and to achieve unity power factor and low distortion currents [9].

This paper is structured as follows. In order to give a clear description of the proposed control method, a complete modelling of WECS is firstly presented in Section 2. In Section 3, control of system will be presented. The simulations results are given in Section 4. Finally, some conclusions are presented in Section 5.

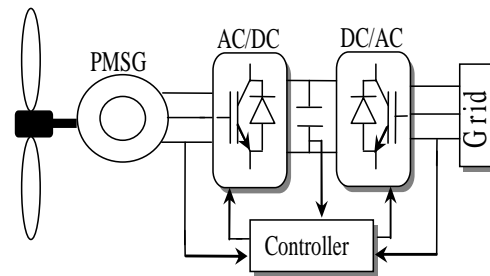


Fig.1. Block diagrams of WECS.

2. MODELING OF WECS

2.1. Wind Turbine Characteristic

A wind turbine can't fully capture wind energy. So, the components of wind turbine have been modelled by the following equations. The output power of the wind-turbine is expressed as [3]:

$$P_{Turbine} = \frac{1}{2} \rho A C_p(\lambda, \beta) v^3 \quad (1)$$

where, ρ is the air density (typically 1.225 kg/m^3), A is the area swept by the rotor blades (in m^2), C_p is the coefficient of power conversion which depend on the wind characteristic and its operating point and v is the wind speed (in m/s). Consequently, the output power of the wind turbine is determined by the power coefficient if the swept area, air density, and wind velocity are constant. The coefficient of performance of a wind turbine is influenced by the tip-speed ratio, which is defined as [2]:

$$\lambda = \frac{\omega_m R}{v} \quad (2)$$

where R and ω_m are the rotor radius (in m) and rotor angular velocity (in rad/sec), respectively.

The wind turbine mechanical torque output T_m given as:

$$T_m = \frac{1}{2} \rho A C_p(\lambda, \beta) v^3 \frac{1}{\omega_m} \quad (3)$$

A generic equation is used to model the coefficient of power conversion $C_p(\lambda, \beta)$ based on the modelling turbine characteristics described in [2] and [10] as:

$$C_p = \frac{1}{2} \left(\frac{116}{\lambda_i} - 0.4\beta - 5 \right) e^{-\left(\frac{21}{\lambda_i}\right)} \quad (4)$$

$$\frac{1}{\lambda_i} = \frac{1}{\lambda + 0.08\beta} - \frac{0.035}{\beta^3 + 1}$$

The $C_p(\lambda, \beta)$ characteristics, for various values of the pitch angle β , are illustrated in Fig 2. The coefficient of power conversion and so the power are maximum at a certain value of tip speed ratio called optimum tip speed ratio λ_{opt} . The maximum value of $C_p(\lambda, \beta)$, that is $C_{p_{max}} = 0.41$, is achieved for $\lambda_{opt} = 8.1$ and for $\beta = 0^\circ$. Then:

$$P_{Turbine} = \frac{1}{2} \rho A C_{p_{max}} v^3 \quad (5)$$

This particular value results in the point of optimal efficiency where the maximum output power is captured from wind by the wind turbine generator. Consequently, for any particular wind speed, there exists a specific point in the wind

generator power characteristic, where the output power is maximized. So, it is necessary to keep the rotor speed at an optimum value of the tip speed ratio, λ_{opt} . Then the system can operate at the peak of the $P(\omega_m)$ curve when the wind speed changes and the maximum power is extracted continuously from the wind (MPPT control) [3], [22]. That's illustrated in Fig.3. Thus, the curve connecting the peaks of these curves will generate the maximum output power for a given wind speed and follows the path for maximum power operation.

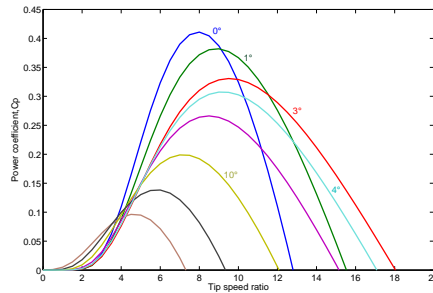


Fig.2. Characteristics C_p vs. λ ; for various values of the pitch angle β

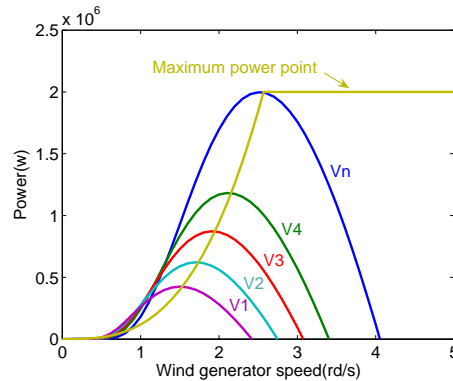


Fig.3. Wind generator power curves at various wind speed

2.2. Modelling of PMSG

Dynamic modelling of PMSG can be described in synchronous rotating reference frame where the q-axis is 90° ahead of the d-axis with respect to the direction of rotation. Thus, it is given by the following equations [15], [18]:

$$v_{gq} = R_g i_q + L_q \frac{di_q}{dt} + \omega_e L_d i_d + \omega_e \psi_f \quad (6)$$

$$v_{gd} = R_g i_d + L_d \frac{di_d}{dt} - \omega_e L_q i_q \quad (7)$$

where L_q and L_d are the inductances of the generator on the q and d axis, R_g is the stator resistance, ψ_f is the permanent magnetic flux and ω_e is the electrical rotating speed of the PMSG, defined as:

$$\omega_e = p_n \omega_m \quad (8)$$

where p_n is the number of pole pairs of the PMSG and ω_m is the mechanical angular speed.

In addition, if $i_d = 0$ the expression for the electromagnetic torque in the rotor can be described as [10]:

$$T_e = \frac{3}{2} p_n \psi_f i_q \quad (9)$$

The dynamic equation of the wind turbine is given as:

$$J \frac{d\omega_m}{dt} = T_e - T_m - F \omega_m \quad (10)$$

where J is the total moment of inertia, F is the viscous friction coefficient and T_m is the mechanical torque developed by the turbine.

3. THE CONTROL SYSTEM

3.1. Adopted MPPT Control Strategy

MPPT controller is used in order to generate the reference speed command which will enable the WECS to extract maximum power from the available wind power. In addition, for each instantaneous wind speed, the optimal rotational speed of the wind turbine rotor can be simply estimated as follows [3]:

$$\omega_{opt} = \frac{v \lambda_{opt}}{R} \quad (11)$$

The maximum mechanical output power of the turbine is given as follows:

$$P_{Turbine_max} = \frac{1}{2} \rho A C_p \max \left(\frac{R \omega_{opt}}{\lambda_{opt}} \right)^3 \quad (12)$$

Thus, we can get the maximum power $P_{Turbine_max}$ by regulating the generator speed in different wind

speed under rated power of the wind power system. The MPPT controller computes this optimum speed and an optimum value of tip speed ratio λ_{opt} can be maintained and maximum wind power can be captured.

3.2. Pitch control

The pitch angle controller can keep the WECS operating at rated active power. So, it's only active in high wind speeds and it's designed to prevent generator power exceeding rated power. Therefore, by reducing the coefficient of power conversion, both the power and rated rotor speed are maintained for above rated wind speeds. So, the blade pitch angle, β , will increase until the wind turbine generator is at the rated speed [9]. The schematic diagram of the implemented turbine blade pitch angle controller is shown in Fig.4. where P is the generated power.

3.3. Nonlinear control of the generator side converter with MPPT and sliding mode control

The adopted MPPT controller generates ω_{m_opt} , the reference speed which when applied to the speed control loop of the generator side converter control system, maximum power will be produced by the WECS. The generator side three-phase converter is used as a rectifier and works as a driver controlling the generator operating at optimum rotor speed ω_{m_opt} in order to obtain maximum energy from wind [9].

In addition, Sliding Mode Control strategy is used. It's deduced from equations (9) and (10) that the wind turbine speed can be controlled by regulating the q-axis stator current components (i_{qr}). So, in order to satisfy the sliding mode condition, define the sliding surface for the speed controller [35]:

$$S_\omega = \omega_{m_opt} - \omega_m \quad (13)$$

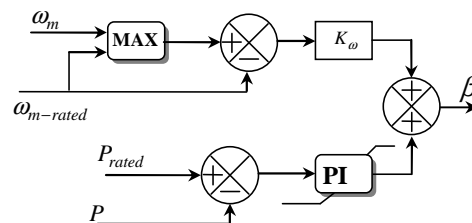


Fig.4. WECS Pitch angle controller.



ω_{m_opt} is generated by a MPPT method. In addition, in order to determine the stabilizing function, the following Lyapunov function is defined as [29]:

$$Y_{\omega} = \frac{1}{2} S_{\omega}^2 \quad (14)$$

Because of the system stability needs to be proven, Lyapunov's stability theory is often deployed, and in order to attract the rotor speed to the reference ω_{m_opt} , the following condition must be fulfilled [32-34]:

$$\dot{Y}_{\omega} = S_{\omega} \dot{S}_{\omega} < 0 \quad (15)$$

In addition, when the sliding mode occurs on the sliding surface, then:

$$S_{\omega} = \dot{S}_{\omega} = 0 \quad (16)$$

In order to obtain commutation around the surface and good dynamic performances, the control includes two terms [32]:

$$u_c = u_{eq} + u_n \quad (17)$$

u_{eq} is an equivalent control input that determines the system's behavior on the sliding surface. In addition, it's the estimated equivalent control used to compensate the unknown system dynamics. During the sliding mode and in permanent regime, u_{eq} is calculated from the expression:

$$\dot{S}_{\omega} = 0 \quad (18)$$

u_n is used in order to guarantee the attractiveness of the variable to be controlled towards the commutation surface. It maintains the state on the sliding surface in the presence of the parameter variations and disturbances. Then

$$u_n = k_{\omega} \text{sgn}(S_{\omega}) \quad (19)$$

where $k_{\omega} > 0$.

Nonlinear control Sliding Mode is a discontinuous control. In order to reduce the chattering, the continuous function as exposed in (20) where $\text{sgn}(S_{\omega})$ is a sign function defined as [31]:

$$\text{sgn}(S_{\omega}) = \begin{cases} 1 & S_{\omega} > \varepsilon \\ \frac{S_{\omega}}{\varepsilon} & \varepsilon \geq |S_{\omega}| \\ -1 & -\varepsilon > S_{\omega} \end{cases} \quad (20)$$

ε is a small positive number. If the ε is too small or too large, the dynamic quality of the system will be reduced. After that, the value of ε should be chosen vigilantly [31].

Therefore, in order to reduce the copper loss by setting the d axis current to be zero and to ensure the PMSG speed convergence to the optimum speed, currents references are derived. The following equation for the system speed is obtained from equations (9), (10), (16), (17), (18), (19) and (20):

$$i_{dr} = 0 \quad (21)$$

$$i_{qr} = \frac{2}{3p_n \psi_f} (T_m + J \dot{\omega}_{m_opt} + F \omega_m + k_{\omega} \text{sgn}(S_{\omega})) \quad (22)$$

By differentiating the Lyapunov function (14), we obtain:

$$\begin{aligned} \dot{Y}_{\omega} &= S_{\omega} \dot{S}_{\omega} \\ &= -\mu_{\omega} S_{\omega}^2 + \frac{S_{\omega}}{J} (\omega_{m_opt} + T_m + F \omega_m \\ &\quad - \frac{3p_n \psi_f i_{qr}}{2} + \mu_{\omega} J S_{\omega}) \end{aligned} \quad (23)$$

where $\mu_{\omega} > 0$

So, with (22), (23) becomes

$$\dot{Y}_{\omega} = -\mu_{\omega} S_{\omega}^2 < 0 \quad (24)$$

Thus, achieving global asymptotical stability.

Using the Lyapunov's direct method, since Y_{ω} is clearly positive definite, \dot{Y}_{ω} is negative definite and Y_{ω} tends to infinity as S_{ω} tends to infinity, then the equilibrium at the origin $S_{\omega} = 0$ is globally asymptotically stable. Thus S_{ω} tends to zero as the time tends to infinity. Moreover, all trajectories starting off the sliding surface $S_{\omega} = 0$ must reach it in a limited time and then will remain on this surface.

In addition, a sliding mode control is used in order to regulate the currents to their references.

A. q-axis current controller design:

Q-axis current controller is used in order to achieve i_{qr} , the desired values of q- axis current. So



we define the sliding surface, for the current component i_q , as follows[34-35]:

$$S_q = i_{qr} - i_q \quad (25)$$

It follows that:

$$\dot{S}_q = \dot{i}_{qr} - \dot{i}_q \quad (26)$$

when the sliding mode occurs on the sliding surface, then:

$$S_q = \dot{S}_q = 0 \quad (27)$$

In order to obtain good dynamic performances and commutation around the surface, the control includes two terms:

$$v_{qr} = v_{eq-q} + v_{n-q} \quad (28)$$

Combing (6), (25), (26), (27) and (28) the controls voltage of q axis is defined by:

$$v_{eq-q} = R_g i_q + L_d \omega_e i_d + \omega_e \psi_f + L_q \dot{i}_{qr} \quad (29)$$

$$v_{n-q} = k_q \text{sgn}(S_q) \quad (30)$$

where $k_q > 0$.

Theorem 1: If the Dynamic sliding mode control laws are designed as (28), (29) and (30), therefore the global asymptotical stability is ensured.

The proof of the theorem 1 will be carried out using the Lyapunov stability theory.

Proof: To determine the required condition for the existence of the sliding mode, it is necessary to design the Lyapunov function. So, we can define a new function of Lyapunov including the q axis current as:

$$Y_q = \frac{1}{2} S_q^2 \quad (31)$$

From Lyapunov stability theory, in order to guarantee the attraction of the system throughout the surface [33], Y_q can be derived that,

$$\dot{Y}_q < 0 \quad (32)$$

By differentiating the Lyapunov function (31), we obtain:

$$\dot{Y}_q = S_q \dot{S}_q \quad (34)$$

So, with (29) and (30) the following inequality is satisfied:

$$\dot{Y}_q = -\mu_q S_q^2 < 0 \quad (35)$$

where $\mu_q > 0$.

B. d-axis current controller design

In order to reduce the copper loss, the objective of d-axis current controller is to keep the current on the d-axis to be zero. Let us introduce the following sliding surface for the current components i_d :

$$S_d = i_{dr} - i_d \quad (36)$$

It follows that:

$$\dot{S}_d = \dot{i}_{dr} - \dot{i}_d \quad (37)$$

when the sliding mode occurs on the sliding surface, then:

$$S_d = \dot{S}_d = 0 \quad (38)$$

the control includes two terms in order to obtain commutation around the surface and good dynamic performances :

$$v_{dr} = v_{eq-d} + v_{n-d} \quad (39)$$

Combing (7), (36), (37), (38) and (39) the controls voltage of d axis is defined by:

$$v_{eq-d} = R_g i_d - L_q \omega_e i_q \quad (40)$$

$$v_{n-d} = k_d \text{sgn}(S_d) \quad (41)$$

where $k_d > 0$.

Theorem 2: If the Dynamic sliding mode control laws are designed as (39), (40) and (41), then the global asymptotical stability is ensured.

Proof: According to Lyapunov stability theorem, the Lyapunov function, including the d axis current, is written as:

$$Y_d = \frac{1}{2} S_d^2 \quad (42)$$

For stability to the switching surface, it is sufficient to have :

$$\dot{Y}_d < 0 \quad (43)$$

By differentiating the Lyapunov function (42), we obtain:

$$\dot{Y}_d = S_d \dot{S}_d \quad (44)$$

So, with (40) and (41) the following inequality is satisfied:

$$\dot{Y}_d = -\mu_d S_d^2 < 0 \quad (45)$$

where $\mu_d > 0$.

Thus, the global asymptotical stability is ensured and the speed control tracking is achieved.

At last, PWM is used in order to produce the control signal to implement the nonlinear control for the generator. The double closed-loop control diagram for generator-side converter is shown as Fig.5.

3.4. Grid-Side Controller Methodology and implementation

The grid side converter feeds generated energy into the grid, keeps the DC link voltage stable and adjusts the quantity of the reactive and active powers delivered to the grid during wind variation or load transients. There are many strategies used to control grid side converter [16]. In this paper, the SM controllers are used to regulate the output voltage and currents in the inner control loops and the DC voltage controller in the second loop (Fig.6).

The voltage balance across the inductor L_f is given by [20]:

$$\begin{bmatrix} e_a \\ e_b \\ e_c \end{bmatrix} = R_f \begin{bmatrix} i_a \\ i_b \\ i_c \end{bmatrix} + L_f \frac{d}{dt} \begin{bmatrix} i_a \\ i_b \\ i_c \end{bmatrix} + \begin{bmatrix} v_a \\ v_b \\ v_c \end{bmatrix} \quad (46)$$

where L_f and R_f are the filter inductance and resistance respectively; e_a , e_b and e_c represent voltages at the inverter output; v_a , v_b and v_c represent the grid voltage components voltages; i_a , i_b and i_c are the line currents. Transformation in the rotating dq reference frame is calculated as follows:

$$v_d = e_d - R_f i_{d-f} - L_f \frac{di_{d-f}}{dt} + \omega L_f i_{q-f} \quad (47)$$

$$v_q = e_q - R_f i_{q-f} - L_f \frac{di_{q-f}}{dt} - \omega L_f i_{d-f} \quad (48)$$

where e_d and e_q are the inverter d-axis q-axis voltage components respectively. i_{d-f} and i_{q-f} are the d-axis current and q-axis current of Grid. v_d

and v_q are the grid voltage components in the d-axis q-axis voltage components respectively.

The DC-side equation can be given by:

$$C \frac{dU_{dc}}{dt} = \frac{3}{2} \left(\frac{v_d}{U_{dc}} i_{d-f} + \frac{v_q}{U_{dc}} i_{q-f} \right) - i_{dc} \quad (49)$$

where i_{dc} and U_{dc} are the DC-bus current and DC-bus voltage respectively.

The instantaneous power is given by [20]:

$$Q = \frac{3}{2} (v_d i_{q-f} - v_q i_{d-f}) \quad (50)$$

$$P = \frac{3}{2} (v_d i_{d-f} + v_q i_{q-f}) \quad (51)$$

If the grid voltage space vector \vec{u} is oriented on d-axis, then:

$$\begin{aligned} v_d &= V \\ v_q &= 0 \end{aligned} \quad (52)$$

Thus, equations (47-48) may be expressed as:

$$L_f \frac{di_{d-f}}{dt} = e_d - R_f i_{d-f} + \omega L_f i_{q-f} - V \quad (53)$$

$$L_f \frac{di_{q-f}}{dt} = e_q - R_f i_{q-f} - \omega L_f i_{d-f} \quad (54)$$

Then, the reactive power and active power can be expressed as:

$$P = \frac{3}{2} V i_{d-f} \quad (55)$$

$$Q = \frac{3}{2} V i_{q-f} \quad (56)$$

Therefore, reactive and active power control can be achieved by controlling quadrature and direct current components, respectively. In addition, basically, the aim of the control, of the grid side, is to transfer all the active power produced by the PMSG to the grid and also to produce no reactive power so that unity power factor is obtained. So, the DC-link voltage must remain constant.

The d-axis reference current is determined by DC-link voltage controller in order to control the converter output real power [10], [20]. There are two closed-loop controls for the power converter. The fast dynamic is associated with the line current

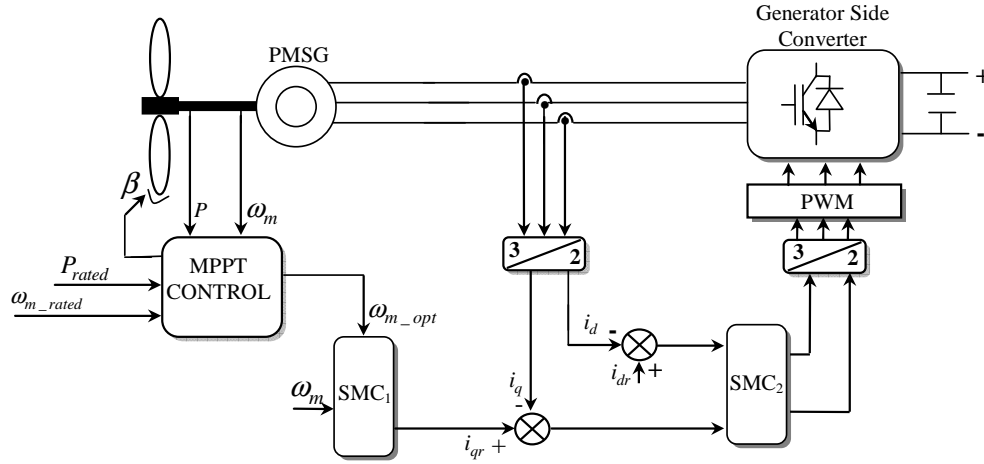


Fig.5. Block diagram of machine side converter controller

control in the inner loop where the nonlinear SM control is adopted to track the line current control, but in the outer loop slow dynamic is associated with the DC voltage control. In addition, the PI regulator is employed in order to generate the reference source current i_{dr-f} and regulate the DC voltage, but the reference signal of the q-axis current i_{qr-f} is produced by the reactive power Q_r according to (56).

A. d-axis current controller design

The objective of d-axis current controller is to keep the current on the d-axis to be i_{dr-f} . In addition, the current i_{dr-f} is provided from a DC-link voltage control block. Let us introduce the following sliding surface for the current component i_{d-f} :

$$S_{d-f} = i_{dr-f} - i_{d-f} \quad (57)$$

where i_{dr-f} is the desired value of d-axis current

It follows that:

$$\dot{S}_{d-f} = \dot{i}_{dr-f} - \dot{i}_{d-f} \quad (58)$$

when the sliding mode occurs on the sliding surface, then:

$$S_{d-f} = \dot{S}_{d-f} = 0 \quad (59)$$

The proposed sliding mode controller contains two parts, in order to obtain commutation around the surface and good dynamic performances [32]:

$$v_{dr-f} = v_{eq-d-f} + v_{n-d-f} \quad (60)$$

Combining (53), (57), (58), (59) and (60) the controls voltage of d axis is defined by:

$$v_{eq-d-f} = L_f \frac{di_{dr-f}}{dt} + R_f i_{d-f} - L_f \omega i_{q-f} + V \quad (61)$$

$$v_{n-d-f} = k_{d-f} \text{sgn}(S_{d-f}) \quad (62)$$

where $k_{d-f} > 0$.

Theorem 3: If the Dynamic sliding mode control laws are designed as (60), (61) and (62), then the global asymptotical stability is ensured.

Proof: Having proposed sliding surface S_{d-f} , the control algorithm should be designed such that vector S_{d-f} is reduced to zero after a limited time.

So, we can define a new function of Lyapunov including the d axis current as:

$$Y_{d-f} = \frac{1}{2} S_{d-f}^2 \quad (63)$$

From Lyapunov stability theory, in order to guarantee the attraction of the system throughout the surface and the sliding manifold is reached after a limited time, Y_{d-f} can be derived that:

$$Y_{d-f} \dot{< 0 \quad (64)$$

By differentiating the Lyapunov function (63), we obtain:

$$\dot{Y}_{d-f} = S_{d-f} \dot{S}_{d-f} \quad (65)$$

So, with (61) and (62) the following inequality is satisfied:

$$\dot{Y}_{d-f} = -\mu_{d-f} S_{d-f}^2 < 0 \quad (66)$$

where $\mu_{d-f} > 0$.

B. q-axis current controller design

The reference signal of the q-axis current is directly given from the outside of the controller and it sets to zero in order to achieve unity power factor control. Let us introduce the following sliding surface for the current component i_{q-f} :

$$S_{q-f} = i_{qr-f} - i_{q-f} \quad (67)$$

where i_{qr-f} is the desired value of q- axis current . So:

$$\dot{S}_{q-f} = \dot{i}_{qr-f} - \dot{i}_{q-f} \quad (68)$$

when the sliding mode occurs on the sliding surface, then:

$$\dot{S}_{q-f} = \dot{S}_{q-f} = 0 \quad (69)$$

To satisfy the stability equation and to get a sliding mode control, a possible control variable can be given as:

$$v_{qr-f} = v_{eq-q-f} + v_{n-q-f} \quad (70)$$

Combing (54), (67), (68), (69) and (70) the controls voltage of q axis is defined by:

$$v_{eq-q-f} = R_f i_{q-f} + L_f \omega i_{d-f} \quad (71)$$

$$v_{n-q-f} = k_{q-f} \text{sgn}(S_{q-f}) \quad (72)$$

where $k_{q-f} > 0$.

Theorem 4: If the Dynamic sliding mode control laws are designed as (70), (71) and (72), then the global asymptotical stability is ensured.

Proof: In order to determine the existence condition of the sliding mode, it's necessary to design the Lyapunov function. So, we can define a new function of Lyapunov including the q axis current as:

$$Y_{q-f} = \frac{1}{2} S_{q-f}^2 \quad (73)$$

To ensure the existence of sliding mode operation,

the local reachability condition must be satisfied

$$\dot{Y}_{q-f} < 0 \quad (74)$$

By differentiating the Lyapunov function (64), we obtain:

$$\dot{Y}_{q-f} = S_{q-f} \dot{S}_{q-f} \quad (75)$$

So, with (71) and (72) the following inequality is satisfied:

$$\dot{Y}_{q-f} = -\mu_{q-f} S_{q-f}^2 < 0 \quad (76)$$

where $\mu_{q-f} > 0$.

So, the asymptotic stability in the current loop is guaranteed. Thus, the DC-link voltage control tracking is achieved.

Finally, PWM is used in order to produce the control signal. The structure of the DC-link voltage and current controllers for grid-side converter is shown in Fig.6.

4. SIMULATIONS RESULTS

This paragraph presents the simulated responses of the WECS under variable wind speed. The parameters of PMSG used are given in Table I and Table II. The block diagram of WECS is shown in Fig.7. During the simulation, the d axis command current of the PMSG side converter control system, i_{dr} , is set to zero; whereas, for the grid side inverter, the q axis command current, i_{qr-f} , is set to zero. Simulation results are given in Fig.8 to Fig. 17. Fig.8-9-10-11-12 show the waveforms of wind speed, tip speed ratio, pitch angle, coefficient of power conversion, aerodynamic power, rotor angular velocity and optimum speed ω_{m_opt} . It can be seen that the wind speed increases, the rotor angular velocity increases proportionally too, the power coefficient will drop to maintain the rated output power. The WECS operate under MPPT control. The initial pitch angle β keeps the value of 0° , the tip speed ratio λ maintains the optimal value 8.1, and the power coefficient C_p is the maximum around 0.41. Although, when the wind speed is up the rated wind speed ($v_n = 12.4\text{m/s}$), the operation of the pitch angle control is actuated and the pitch angle β increase which has for consequence decreasing power coefficient C_p and the tip speed ratio is decreasing. The pitch angle rises to lower the extracted wind power.

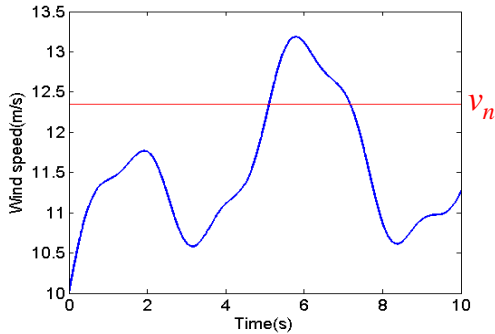


Fig.8. Instantaneous wind speed (m/s)

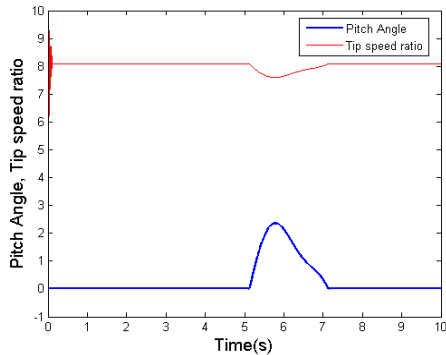


Fig.9. Pitch angle β (in degree) and tip speed ratio λ waveforms.

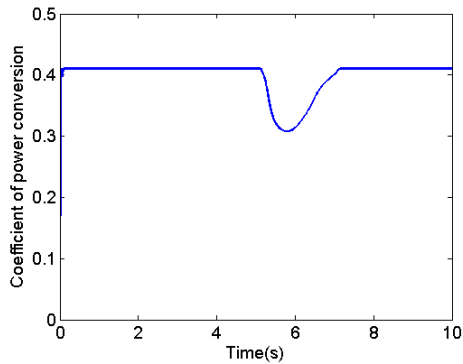


Fig.10. variation of coefficient of power conversion C_p .

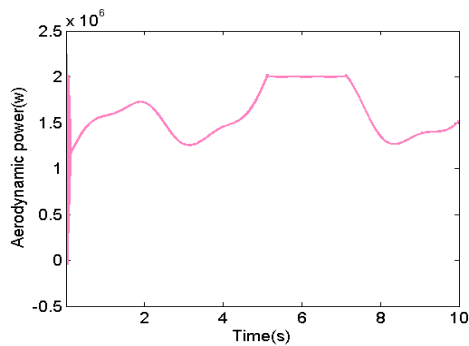


Fig.11. Aerodynamic power (w).

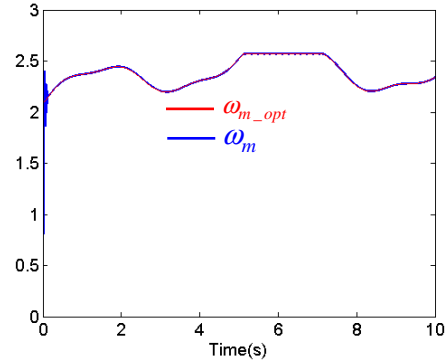


Fig.12. Optimum speed ω_{m_opt} and generator speed ω_m (rd/s).

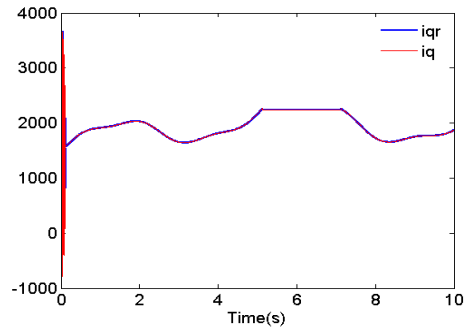


Fig.13. q- axis current component of PMSG i_q and the desired values i_{qr} (A).

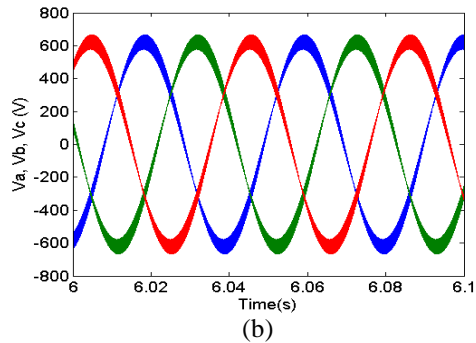
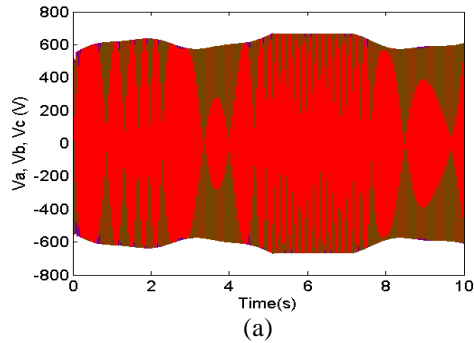


Fig. 14. The waveforms of three phase voltage of PMSG.

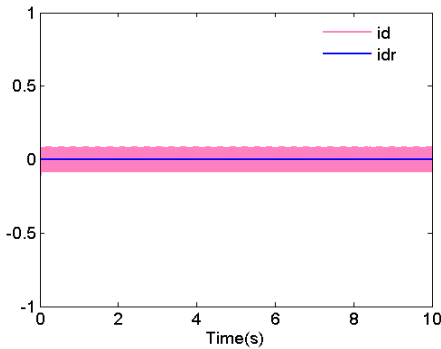


Fig.15. d- axis current component of PMSG i_d and the desired values i_{dr} (A).

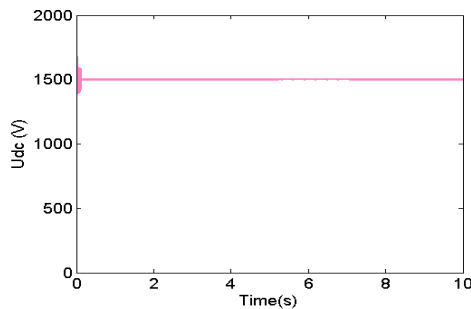


Fig. 16. DC link voltage.

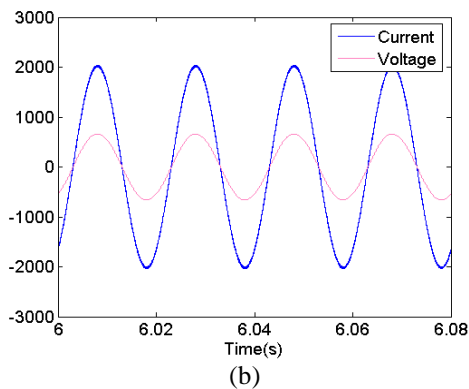
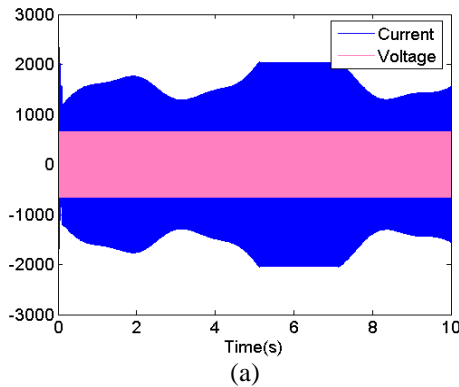


Fig. 17. The waveforms of three phase current and voltage of GRID

5. CONCLUSIONS

This paper has presented the new control of WECS based on Grid connected PMSG. Control algorithm based on the sliding mode strategy has been investigated for the system. The conditions for the existence of the SM are found by using the stability conditions of Lyapunov. Moreover, the concept of MPPT has been presented in terms of the adjustment of the PMSG rotor speed according to instantaneous wind speed and limitation by Pitch angle strategy for high wind speed. Two control schemes at both generator side and grid side converters are implemented. The speed control is realized through SM nonlinear control where the q-axis current is used to control the rotational speed of the generator according to the variation of wind speed. In addition, using SM method, the inverter is controlled to maintain the DC-bus voltage and regulate the grid-side power factor. Thus, the WECS with the PMSG can not only capture the maximum wind power, but also can maintain the frequency and amplitude of the output voltage with unity power factor. Finally, simulation results show clearly that the proposed non linear SM controllers are quite efficient for the WECS and demonstrated the effectiveness and applicability of the proposed control design.

Appendix

TABLE I
PARAMETERS OF THE TURBINE

Parameter	Value
ρ the air density	1.08kg/m ³
A area swept by blades	4775.94 m ²
v_n base wind speed	12.4 m/s

TABLE II
PARAMETERS OF THE POWER SYNCHRONOUS GENERATORS

Parameter	Value
P_r rated power	2 (Mw)
ω_m rated mechanical speed	2.57 (rd/s)
R stator resistance	0.008(Ω)
L_d stator d-axis inductance	0.0003 (H)
L_q stator q-axis inductance	0.0003 (H)
ψ_f permanent magnet flux	3.86 (wb)
p_n pole pairs	60



REFERENCES:

- [1] P.K. Goel, B. Singh, S.S. Murthy, S.K. Tiwari, "Parallel Operation of Permanent Magnet Generators in Autonomous Wind Energy Conversion System", *Proceedings of Industry Applications Society Annual Meeting IAS-IEEE Conferences*, pp.1 - 8, 2010.
- [2] M.A. Abdullah, A.H.M. Yatim, Chee Wei Tan, "A study of maximum power point tracking algorithms for wind energy system", *Proceedings of Clean Energy and Technology (CET), IEEE First Conference on*, pp. 321 - 326, 2011.
- [3] S. M. Muyeen, Rion Takahashi, Toshiaki Murata and Junji Tamura, "A Variable Speed Wind Turbine Control Strategy to Meet Wind Farm Grid Code Requirements", *IEEE Transactions on power systems*, Vol. 25, No. 1, February 2010, pp. 331 - 340.
- [4] Dafeng Fu, Yan Xing, Yundong Ma, "MPPT of VSCF Wind Energy Conversion System Using Extremum Control Strategy", *Proceedings of World Non-Grid-Connected Wind Power and Energy Conference (WNWEC), IEEE Conferences*, pp.1-6, Nov.2010.
- [5] Jinliang Kang, Haifeng Liang; Gengyin Li, Ming Zhou; Hua Yang, "Research on grid connection of wind farm based on VSC-HVDC", *Proceedings of Power System Technology (POWERCON), International Conference on*, pp. 1 - 6, October 2010.
- [6] M.Hilal, M. Maaroufi, M.Ouassaid, "Doubly Fed Induction Generator Wind Turbine Control for a maximum Power Extraction," *Proceedings of International Conference on Multimedia Computing and Systems, IEEE ICMCS'11*, pp. 1-7, 2011.
- [7] Ming Yin, Gengyin Li, Ming Zhou, Guoping Liu, Chengyong Zhao, "Study on the control of DFIG and its responses to grid disturbances," *Power Engineering Society General Meeting, IEEE*, octobere 2006.
- [8] M. Benchagra, M. Maaroufi, M. Ouassaid, "Study and Analysis on the Control of SCIG and its Responses to Grid Voltage Unbalance," *Proceedings of International Conference on Multimedia Computing and Systems, IEEE ICMCS'11*, pp. 1-5, 2011.
- [9] Zhe Chen, Josep M. Guerrero and Frede Blaabjerg, "A Review of the State of the Art of Power Electronics for Wind Turbines," *IEEE Transactions on power electronics*, Vol. 24, No. 8, August 2009, pp. 1859 - 1875.
- [10] Y. Errami, M. Ouassaid and M. Maaroufi, "Modelling and Control Strategy of PMSG Based Variable Speed Wind Energy Conversion System," *Proceedings of IEEE-ICMCS'11*, pp.1-6, 2011.
- [11] A. Mesemanolis, C. Mademlis and I. Kioskeridis, "Maximum Efficiency of a Wind Energy Conversion System with a PM Synchronous Generator," *IEEE-MedPower 2010, Power Generation, Transmission, Distribution and Energy Conversion, Proceedings of 7th Mediterranean Conference and Exhibition on*, pp. 1-9, November 2010.
- [12] F. Blaabjerg, F. Iov, Z. Chen, K. Ma, "Power Electronics and Controls for Wind Turbine Systems", *Energy Conference and Exhibition (EnergyCon), IEEE Conferences*, pp. 333 - 344, December 2010.
- [13] G.Nallavan, R.Dhanasekaran and M.Vasudevan, "Power Electronics in Wind Energy Conversion Systems- A Survey across the Globe", *Proceedings of Electronics Computer Technology (ICECT), IEEE, 3rd International Conference on*, pp. 416 - 419, April 2011.
- [14] K. Kaur, S.Chowdhury, S.P Chowdhury and T.Gaunt, "Fuzzy logic based power optimization of variable speed, variable pitch wind power generation," *Universities Power Engineering Conference UPEC-IEEE, 2009 Proceedings of the 44th International*, pp. 1 - 5.
- [15] Kelvin Tan, and Syed Islam, "Optimum Control Strategies in Energy Conversion of PMSG Wind Turbine System without Mechanical Sensors", *IEEE Transactions On Energy*, Vol. 19, No. 2, June 2004, pp 392 - 399.
- [16] S. M. Muyeen, Rion Takahashi and Junji Tamura, "Operation and Control of HVDC-Connected Offshore Wind Farm", *IEEE Transactions On Sustainable Energy*, Vol. 1, No. 1, April 2010, pp. 30 - 37.
- [17] Gautam Poddar, Aby Joseph, and A. K. Unnikrishnan, "Sensorless Variable-Speed Controller for Existing Fixed-Speed Wind Power Generator With Unity-Power-Factor Operation", *IEEE Transactions On Industrial Electronics*, Vol. 50, No. 5, October 2003, pp. 1007 - 1015.
- [18] L.G. Gonzalez, E. Figueres, G.Garcera, O. Carranza, "Modelling and control in Wind Energy Conversion Systems(WECS)", *Power Electronics and Applications, EPE '09*.



- Proceedings of 13th European Conference on*, pp. 1 - 9, 2009.
- [19] Dafeng Fu, Yan Xing and Yundong Ma, "MPPT of VSCF Wind Energy Conversion System Using Extremum Control Strategy," *Proceedings of World Non-Grid-Connected Wind Power and Energy Conference WNWEC-IEEE*, pp. 1 – 6, November 2010.
- [20] M. E. Haque, K. M. Muttaqi and M. Negnevitsky, "Control of a Stand Alone Variable Speed Wind Turbine with a Permanent Magnet Synchronous Generator," *Proceedings of IEEE Power and Energy Society General Meeting - Conversion and Delivery of Electrical Energy in the 21st Century*, pp.1-9, août 2008.
- [21] Kun Han and Guo-zhu Chen, "A Novel Control Strategy of Wind Turbine MPPT Implementation for Direct-drive PMSG Wind Generation Imitation Platform," *Proceedings of Power Electronics and Motion Control Conference, IPEMC '09. IEEE 6th International*, pp. 2255 – 2259, 2009.
- [22] S. M. Muyeen, Rion Takahashi, Toshiaki Murata and Junji Tamura, "A Variable Speed Wind Turbine Control Strategy to Meet Wind Farm Grid Code Requirements ," *IEEE Transactions On Power systems*, Vol. 25, No. 1, February 2010, pp. 331 – 340.
- [23] Lili Huang, Xin Chen , Lan Xiao and Chunying Gong , "Research on the bi-directional AC-DC converter for the large-scale non-grid-connected wind power application," *Proceedings of World Non-Grid-Connected Wind Power and Energy Conference, WNWEC-IEEE* , pp.1 - 6, September 2009.
- [24] F. Valenciaga, P. F. Puleston, P. E. Battaiotto, and R. J. Mantz, "Passivity/ sliding mode control of a stand-alone hybrid generation system," *IEE Proceedings - Control Theory and Applications*, Vol. 147, No. 6, November. 2000, pp. 680-686.
- [25] B. Beltran, T. Ahmed-Ali, and M. E. H. Benbouzid, "Sliding mode power control of variable-speed wind energy conversion systems," *IEEE Transactions on Energy Conversion*, Vol. 23, No. 2, Jun. 2008, pp. 551-558.
- [26] F. Valenciaga and P. F. Puleston, "High-order sliding control for a wind energy conversion system based on a permanent magnet synchronous generator," *IEEE Transactions on Energy Conversion*, Vol. 23, No. 3, Sep. 2008 pp. 860-867.
- [27] B. Beltran, T. Ahmed-Ali, and M. E. H. Benbouzid, "High-order sliding mode control of variable-speed wind turbines," *IEEE Transactions on Industrial electronics*, Vol. 56, No. 9, September 2009, pp. 3314-3321.
- [28] B. Wang and S. Qin, "Backstepping sliding mode control of variable pitch wind power system," in *Proc. 2010 Asia-Pacific Power and Energy Engineering Conference*, Mar. 28-31, 2010.
- [29] Utkin V. I, "Sliding mode control design principles and applications to electrical drives," *IEEE Trans. on Industrial Electronics*, vol. 40, No. 1, February 1993.
- [30] J. E Slotine and Li W, "Applied Nonlinear Control," Prentice Hall, Englewood Cliffs, New Jersey, 1991.
- [31] Shaojing Wen and Fengxiang Wang, "Sensorless Direct Torque Control of High Speed PMSM Based on Variable Structure Sliding Mode," *Proceedings of Electrical Machines and Systems, ICEMS-IEEE, International Conference on* , pp. 995 – 998, 2008.
- [32] Kairous Djilali, Wamkeue Rene and Belmadani, Bachir, "Advanced Control of Variable Speed Wind Energy Conversion System with DFIG," Environment and Electrical Engineering (EEEIC), *Proceedings of 9th International Conference on* , pp. 41 – 44, 2010.
- [33] A. Hemdani, M.J Ghorbal, M.W. Naouar and I. Slama-Belkhdja, "Design of a switching table for direct power control of a DFIG using sliding mode theory," *Systems, Signals and Devices SSD-IEEE, Proceedings of 8th International Multi-Conference on* , pp. 1 - 7, March 2011.
- [34] Djilali Kairous and René Wamkeue , "Sliding-Mode Control Approach for direct power control of WECS based DFIG," *Proceedings of Environment and Electrical Engineering EEEIC-IEEE, 10th International Conference on* ,pp. 1 – 4, Mai 2011.
- [35] Cheng-Kai Lin, Tian-Hua Liu and Li-Chen Fu, " Adaptive Backstepping PI Sliding-Mode Control for Interior Permanent Magnet Synchronous Motor Drive Systems ," *Proceedings of American Control Conference on ACC-IEEE*, pp. 4075 - 4080 June - July , 2011.